

Sub-diffusive phases in open clean long-range systems

Archak Purkayastha,^{1,*} Madhumita Saha,^{2,†} and Bijay Kumar Agarwalla^{2,‡}

¹*Department of Physics, Trinity College Dublin, Dublin, Ireland*

²*Department of Physics, Indian Institute of Science Education and Research Pune, Dr. Homi Bhabha Road, Ward No. 8, NCL Colony, Pashan, Pune, Maharashtra 411008, India*
(Dated: April 26, 2022)

We show that a one-dimensional ordered fermionic lattice system with power-law-decaying hopping, when connected to two baths at its two ends with different chemical potentials, features two phases with sub-diffusive particle transport at zero temperature. These phases have no analogues in the isolated system (i.e, in absence of the baths) where the transport is perfectly ballistic. In the open system scenario, interestingly, there occurs two chemical potential driven sub-diffusive to ballistic phase transitions at zero temperature. We provide a clear understanding of the microscopic origin of these phases. Moreover, we argue that these sub-diffusive phases are robust against the presence of arbitrary number-conserving many-body interactions in the system. Furthermore, we discuss how this phase transition, to our knowledge, is different from all the known non-equilibrium quantum phase transitions.

Introduction — Understanding transport properties of quantum systems is extremely important both from the fundamental and the application perspective. In fact, fundamental understanding can potentially accelerate device engineering leading to designing efficient thermoelectric generators, quantum heat engines, refrigerators, diodes etc [1–4]. It is now clear that in low-dimensional systems transport properties can deviate significantly from the usual diffusive behaviour [5–7]. One of the most intriguing feature of this is the slower than diffusive or the sub-diffusive transport. This often occurs in quantum systems at the critical region (or point) separating localized and delocalized phases. For example, this is the case for disordered interacting one-dimensional systems where the sub-diffusion is thought to originate from rare occurrence of ordered regions, also known as the Griffiths effect [8–13]. This picture however does not carry over to quasi-periodic systems which lacks disorder. Non-interacting (i.e., quadratic Hamiltonian) quasi-periodic systems like the Aubry-Andre-Harper model [14–17] also shows sub-diffusion at the critical point between the localization-delocalization transition. On the other hand, there are other quasi-periodic potentials, like the Fibonacci potential [18–20], which show a smooth crossover into a sub-diffusive region. In such non-interacting quasi-periodic systems, the sub-diffusive behavior is thought to be related with the fractal properties of the single-particle spectrum and eigenstates [20–23]. The sub-diffusive behavior of quasi-periodic systems has been shown to survive in presence of interactions [23–26] in some cases, though its origin often lacks a general understanding. It is therefore reasonable to state that a clear microscopic understanding of the origin of sub-diffusive transport has remained as a challenging problem.

Importantly, all of the above known examples of sub-diffusive transport require presence of either disorder or quasi-periodicity, and this is usually considered a necessary condition for slow sub-diffusive transport. In this

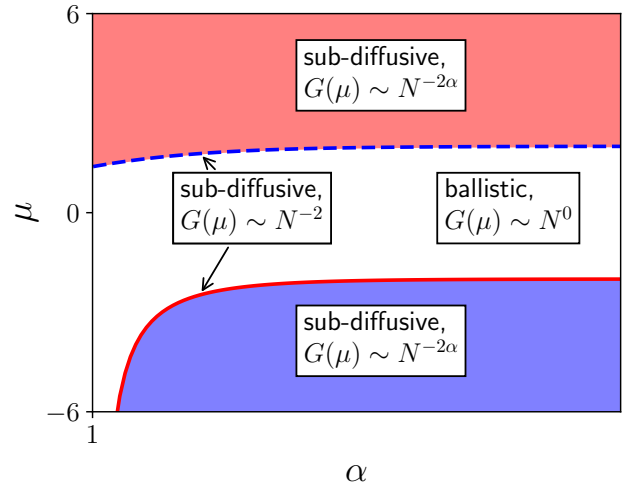


FIG. 1. Non-equilibrium phase diagram obtained from system size scaling of zero-temperature conductance $G(\mu)$ as a function of chemical potential μ and long-range hopping exponent α for one-dimensional open clean long range system (Eq. (1)). We observe two chemical potential driven sub-diffusive to ballistic phase transitions (Eq. 4) which have no corresponding isolated system analogue. The critical lines correspond to the system band edges for $\mu = 2\eta(\alpha)$ (blue dashed line), where $\eta(\alpha)$ is Dirichlet-eta function and $\mu = -2\zeta(\alpha)$ (red line), where $\zeta(\alpha)$ the Riemann-zeta function.

letter, to the contrary, we show, and provide a clear microscopic understanding of the fact that a clean (i.e, ordered) one-dimensional fermionic system with long-range hopping decaying as a power-law can feature two sub-diffusive phases at zero temperature when connected to two baths at its two ends. These sub-diffusive regions emerge due to a non-analyticity of the energy dispersion relation located at the bottom of the system band. Furthermore, these phases do not have any analog in the isolated system, i.e, in absence of the baths, where

the transport is known to be perfectly ballistic [27]. In presence of the baths, however, there occurs two chemical potential driven quantum (i.e., zero temperature) non-equilibrium phase transitions between ballistic and sub-diffusive phases (see Fig. (1)). Moreover, these sub-diffusive phases can be argued to be immune in presence of number-conserving many-body interactions in the system.

Interestingly, one-dimensional long-range lattice systems have received significant attention in recent times due to the possibility of realizing such interactions in an experimentally controlled fashion in several platforms such as Rydberg atoms [28–30], trapped ions [31–39], polar molecules [40–42], dipolar gas [43], nuclear spins [44], nitrogen-vacancy centers in diamond and trapped atoms [45], and demonstrating exotic physics, e.g., time crystals [38, 45], prethermalization [33], dynamical phase transitions [32, 37, 44, 46], environment assisted transport [39] etc. This has lead to interesting set of studies for quantum transport which so far has been limited isolated systems in presence and absence of disorder [27, 47–54], and one spin system with Lindblad boundary-driving [55]. To our knowledge, transport through the long-range systems has not been studied before in a non-Markovian open quantum system setting, as we do here using non-equilibrium-Greens-function (NEGF) and reveal the remarkable sub-diffusive phases with no isolated system analogue.

The clean long-range hopping model — We consider the following one-dimensional lattice model of fermions with long-range hopping decaying as a power-law

$$\hat{\mathcal{H}}_S = - \sum_{m=1}^N \left(\sum_{r=1}^{N-m} \frac{1}{m^\alpha} \left(\hat{c}_r^\dagger \hat{c}_{r+m} + \hat{c}_{r+m}^\dagger \hat{c}_r \right) \right), \quad (1)$$

where \hat{c}_r is the fermionic annihilation operator at the r th site of the system. Interestingly, this long-range model Hamiltonian has recently been realized using Floquet engineering technique in superconducting qubits [56]. The above system Hamiltonian can be written as, $\hat{\mathcal{H}}_S = \sum_{\ell m=1}^N \mathbf{H}_{\ell m} \hat{c}_\ell^\dagger \hat{c}_m$, where the matrix \mathbf{H} is a Toeplitz matrix with elements given by $\mathbf{H}_{\ell m} = \frac{1}{|\ell-m|^\alpha}$, $\forall \ell \neq m$, and $\mathbf{H}_{\ell\ell} = 0$. The eigenspectrum of this matrix, which correspond to the single-particle eigenvalues and eigenvectors of $\hat{\mathcal{H}}_S$, are difficult to find analytically for arbitrary N . But, in the thermodynamic limit, $N \rightarrow \infty$, the single particle eigenvalues can be obtained via a Fourier transform, and correspond to the dispersion relation [57],

$$\varepsilon(k, \alpha) = -2 \sum_{m=1}^{\infty} \frac{\cos(mk)}{m^\alpha}. \quad (2)$$

The infinite series summation in the dispersion relation is absolutely convergent for all k if $\alpha > 1$. It is in this case that the thermodynamic limit ($N \rightarrow \infty$) is well-defined. We will therefore always consider $\alpha > 1$. It can

be numerically verified that the eigenvalues of \mathbf{H} tend to this dispersion relation in the large N limit and the corresponding single-particle eigenvectors of the system are completely delocalized. This property indicates that there should be ballistic transport in the system. Indeed, in the isolated system (under periodic boundary condition) it has recently been shown that the Drude weight is non-zero for all α , which is the hallmark of ballistic transport [27]. On the contrary, as we will show below, in the open system scenario, there is a surprising sub-diffusive to ballistic phase transition as a function of chemical potential for all $\alpha > 1$ at zero temperature. We note that the band-edges of the dispersion relation in Eq.(2) correspond to $\varepsilon(0, \alpha) = -2\zeta(\alpha)$, where $\zeta(\alpha) = \sum_{m=1}^{\infty} \frac{1}{m^\alpha}$ is the Riemann-zeta function, and $\varepsilon(\pm\pi, \alpha) = 2\eta(\alpha)$ with $\eta(\alpha) = \sum_{m=1}^{\infty} \frac{(-1)^{m-1}}{m^\alpha}$ being the Dirichlet eta function.

Open system classification of transport at zero temperature — To classify transport in the open quantum system setting, we consider the two terminal transport set-up where the system is connected to two baths at its two ends, i.e., the first and the N th sites. Such open system set-up is exactly what is used for realizing autonomous (continuous) quantum heat engines and refrigerators, thermoelectric generators etc [58–60]. This classification of transport is therefore directly relevant for these applications. The left (right) bath is modelled by a non-interacting Hamiltonian with an infinite number of modes $\hat{\mathcal{H}}_{B_1} = \sum_{r=1}^{\infty} \Omega_r \hat{B}_{r1}^\dagger \hat{B}_{r1}$ ($\hat{\mathcal{H}}_{B_N} = \sum_{r=1}^{\infty} \Omega_r \hat{B}_{rN}^\dagger \hat{B}_{rN}$), where \hat{B}_{r1} (\hat{B}_{rN}) is the fermionic annihilation operator of the r th mode of the left (right) bath. The baths are connected to the system with the system-bath coupling Hamiltonian $\hat{\mathcal{H}}_{SB} = \sum_{\ell=1, N} \sum_{r=1}^{\infty} (\kappa_{r\ell} \hat{c}_\ell^\dagger \hat{B}_{r\ell} + \kappa_{r\ell}^* \hat{B}_{r\ell}^\dagger \hat{c}_\ell)$. Initially, the baths are assumed to be at their own thermal states with their own temperatures and chemical potentials (μ_1, μ_N), while the system's initial state is arbitrary. We are specifically interested in the non-equilibrium steady state (NESS) in the zero temperature limit and linear response regime, $\mu_1 = \mu$, $\mu_N = \mu - \Delta\mu$, $\Delta\mu \rightarrow 0$.

It is possible to obtain the exact NESS properties of the system using the NEGF approach [61, 62]. The NEGF for such a set-up is given by $\mathbf{G}^+(\omega) = [\omega \mathbb{I} - \mathbf{H} - \Sigma^{(1)}(\omega) - \Sigma^{(N)}(\omega)]^{-1}$, where \mathbb{I} is the N -dimensional identity matrix, and $\Sigma^{(1)}(\omega)$ ($\Sigma^{(N)}(\omega)$) is the self-energy matrix due to the left (right) bath. The only non-zero element in the $N \times N$ left (right) bath self-energy matrix is the top left (bottom right) corner element, $\Sigma_{\ell\ell}^{(\ell)}(\omega) = -i \frac{\Im_\ell(\omega)}{2} - \mathcal{P} \int \frac{d\omega'}{2\pi} \frac{\Im_\ell(\omega')}{\omega - \omega'}$, $\ell = \{1, N\}$. Here \mathcal{P} denotes principal value, and $\Im_\ell(\omega)$ is the bath spectral function, defined as $\Im_\ell(\omega) = 2\pi \sum_{r=1}^{\infty} |\kappa_{r\ell}|^2 \delta(\omega - \Omega_r)$. The zero temperature particle conductance $G(\mu)$ is given in terms of the

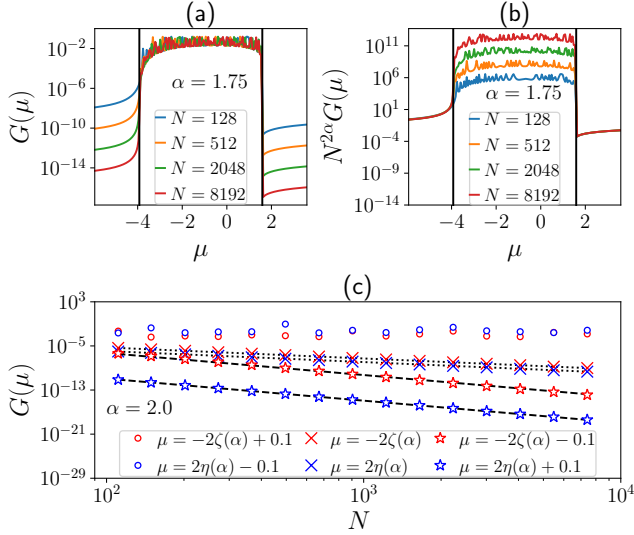


FIG. 2. (a) Zero-temperature conductance $G(\mu)$ as a function of chemical potential μ , at a chosen value of $\alpha = 1.75$ for various system sizes N . The two vertical lines correspond to band-edges $\mu = -2\zeta(\alpha)$ and $\mu = 2\eta(\alpha)$. (b) The same plot as in (a) but with the y-axis scaled by $N^{2\alpha}$. (c) The scaling of $G(\mu)$ with system size at various values of μ , for $\alpha = 2.0$. The black dashed lines are fits of $N^{-2\alpha}$. The black dotted lines are fits of N^{-2} . For the plots, the bath spectral functions are chosen to be $\mathfrak{J}_1(\omega) = \mathfrak{J}_N(\omega) = \Gamma\sqrt{1 - (\frac{\omega}{\Lambda})^2}$, with $\Lambda = 8$, $\Gamma = 10$. All energy scales are in units of nearest neighbour hopping strength.

NEGF as,

$$G(\mu) = \lim_{\Delta\mu \rightarrow 0} \frac{I}{\Delta\mu} = \frac{1}{2\pi} \mathcal{T}(\mu) = \frac{\mathfrak{J}_1(\mu)\mathfrak{J}_N(\mu)|\mathbf{G}_{1N}^+(\mu)|^2}{2\pi}, \quad (3)$$

where $\mathcal{T}(\omega)$ is the transmission function and $I = \int_{\mu_1}^{\mu_N} \frac{d\omega}{2\pi} \mathcal{T}(\omega)$ is the NESS particle current. The scaling of conductance with system-size N is used to classify transport properties. Assuming $G(\mu) \sim N^{-\delta}$, if $\delta = 0$, i.e., conductance is independent of system size, the transport is ballistic. For normal diffusive transport, $\delta = 1$, for super-diffusive transport, $0 < \delta < 1$, while for sub-diffusive transport, $\delta > 1$. If $G(\mu) \sim e^{-N}$, then there is essentially no transport, and it often corresponds to a localized phase.

Chemical potential driven sub-diffusive to ballistic phase transition — We numerically calculate the exact transmission function, and study the conductance scaling with system size. Our central result is as follows. For $1 < \alpha < \infty$,

$$\begin{aligned} G(\mu) &\sim N^{-2\alpha}, \quad \forall \mu < -2\zeta(\alpha), \mu > 2\eta(\alpha), \\ G(\mu) &\sim N^{-2}, \quad \text{at } \mu = -2\zeta(\alpha), 2\eta(\alpha), \\ G(\mu) &\sim N^0, \quad \forall -2\zeta(\alpha) < \mu < 2\eta(\alpha), \end{aligned} \quad (4)$$

where, as mentioned before, $\zeta(\alpha)$ is the Riemann-zeta function and $\eta(\alpha)$ is the Dirichlet-eta function. In other words, when the chemical potential μ is within the band of the system, the transport is ballistic, as expected. But, surprisingly, when μ lies outside the band of the system, the transport is sub-diffusive, with an exponent of 2α . Moreover, when μ is located exactly at the band-edges, the transport is again sub-diffusive but with an α independent exponent. Representative plots showing the above behavior are given in Fig. 2. Fig. 2(a) shows the behavior $G(\mu)$ with μ for various system sizes at a chosen value of α ($\alpha = 1.75$). Clearly, within the band, i.e., $-2\zeta(\alpha) < \mu < 2\eta(\alpha)$, there is no scaling of $G(\mu)$ with N , confirming perfect ballistic behavior, whereas outside that regime $G(\mu)$ scales with system size. Fig. 2(b) shows the same result as in Fig. 2(a) with the y-axis now scaled by $N^{2\alpha}$. All data points outside the band of the system collapse perfectly, thereby confirming the sub-diffusive scaling. Likewise, the α independent scaling at the band-edges can also be checked (not shown in the figure for $\alpha = 1.75$) numerically. Interestingly, this behavior is seen at all values of $\alpha > 1$. Fig 2(c) shows conductance scaling with system size at values close to the system band-edges for a different value of α ($\alpha = 2$). The behavior consistent with Eq.(4) is clearly observed here. Therefore, there is a clear chemical potential driven non-analytic change from sub-diffusive to ballistic behavior occurring at $\mu = -2\zeta(\alpha), 2\eta(\alpha)$.

Origin of the sub-diffusive phases — The origin of these surprising sub-diffusive phases for chemical potentials outside the band of the system can be traced to the non-analyticity property of the dispersion relation at its minimum value at $k = 0$. From Eqs. (3), it is evident that the system size scaling of conductance originates from that of $\mathbf{G}_{1N}^+(\mu)$. Since the baths are attached only to the first and the last sites, we conjecture that, for large N , system size scaling of $\mathbf{G}_{1N}^+(\mu)$ will be same as $\mathbf{g}_{1N}^+(\mu)$, where $\mathbf{g}^+(\mu) = [(\mu - i\epsilon)\mathbb{I} - \mathbf{H}]^{-1}$ is the bare Green's function of the system in absence of the baths. That is, $\mathbf{G}_{1N}^+(\mu) \propto \mathbf{g}_{1N}^+(\mu)$ with the proportionality constant being independent of N . Also, since the system is clean (ordered), in the $N \rightarrow \infty$ limit, one can obtain the bare Green's function via a Fourier transform, $\mathbf{g}_{pq}(\mu) = \lim_{\epsilon \rightarrow 0} \int dk g(k, \omega) e^{-ik|p-q|}$, where $g(k, \mu) = [\mu - \varepsilon(k, \alpha) - i\epsilon]^{-1}$. Combining all of these, we have, for large N ,

$$\mathbf{G}_{1N}^+(\mu) \propto \lim_{\epsilon \rightarrow 0} \int_{-\pi}^{\pi} dk \frac{e^{-ikN}}{\mu - \varepsilon(k, \alpha) - i\epsilon}. \quad (5)$$

The above heuristic expression, in combination with Eq.(3), relates the scaling of conductance with system size of an open system with spectral properties of the isolated system in the thermodynamic limit.

The major contribution to the above integral comes from the singularities of the integrand. It can be checked that $k = 0$ is always a singular point because $\varepsilon(k, \alpha)$ is

non-analytic at $k = 0$, $\lim_{k \rightarrow 0} \frac{\partial^p \varepsilon(k, \alpha)}{\partial k^p} \rightarrow \infty$, $\forall p > \alpha - 1$. To capture the effect of this non-analyticity, we derive a non-trivial non-analytic small k expansion of $\varepsilon(k, \alpha)$ for non-integer $\alpha > 1$ [57],

$$\varepsilon(k, \alpha) \simeq -2 [\zeta(\alpha) - a_1 |k|^{\alpha-1} - a_2 k^2], \quad \forall |k| \ll 1 \quad (6)$$

where a_1 and a_2 are real numbers. The presence of $|k|^{\alpha-1}$ makes the above expression explicitly non-analytic, clearly distinguishing it from a standard Taylor expansion. While evaluating the integral in Eq.(5) via contour integration, the non-integer value of α leads to a branch whose contribution to Eq.(5) can be shown to scale with system-size as $N^{-\alpha}$ [57]. Though these results are obtained for non-integer values of α , integer values of α can be included by assuming an arbitrarily small fractional part.

Now, when μ is within the band of the system, $-2\zeta(\alpha) < \mu < 2\eta(\alpha)$, there are additional poles on the real line. It can be checked easily that such poles can at best generate an oscillatory behavior with N and thus cannot provide a scaling with N . These poles within the band therefore gives the leading behavior $\mathbf{G}_{1N}^+(\mu) \sim N^0$ implying ballistic transport. When μ is below the band of the system, i.e., $\mu < -2\zeta(\alpha)$, the main contribution to the integral with respect to system size comes from the non-analytic point $k \rightarrow 0$. As mentioned above, in this case, the contour integration generates a scaling of the form $\mathbf{G}_{1N}^+(\mu) \sim N^{-\alpha} \quad \forall \mu < -2\zeta(\alpha)$, leading to a sub-diffusive exponent of 2α from Eq.(3). On the other hand, when $\mu > 2\eta(\alpha)$, one may argue that the main contribution to the integral comes from $k \sim \pm\pi$ corresponding to the upper band edge, $\varepsilon(\pm\pi, \alpha) = 2\eta(\alpha)$, where the denominator in Eq.(5) would be minimum. However, an expansion about this point, $\varepsilon(k \pm \pi, \alpha) \simeq 2\eta(\alpha) - 2a_2(1 - 2^{3-\alpha})k^2$, $|k| \ll 1$, shows that, unlike the lower band edge at $k = 0$, this point is analytic, and its contribution to the integral in Eq.(5) decays exponentially with N [57]. Consequently, for large enough N , the leading contribution once again stems from the singularity at $k = 0$, and giving $\mathbf{G}_{1N}^+(\mu) \sim N^{-\alpha} \quad \forall \mu > 2\eta(\alpha)$, leading to the same sub-diffusive exponent. However, interestingly, since the denominator in Eq.(5) is now large, the value of $\mathbf{G}_{1N}^+(\mu)$, and therefore the conductance, for $\mu > 2\eta(\alpha)$ is much smaller than that for $\mu < -2\eta(\alpha)$, even though the system size scaling is the same. This is clearly seen in all the plots of Fig. 2.

A more careful analysis is required at the critical points $\mu = -2\zeta(\alpha), 2\eta(\alpha)$. Note that, at any finite N , the critical μ values always lie slightly outside the system band, but the minimum and maximum eigenvalues of \mathbf{H} approach these values in the thermodynamic limit $N \rightarrow \infty$. We find that it becomes difficult to use Eq.(5) to capture this behavior. Nevertheless, the conjecture $\mathbf{G}_{1N}^+(\mu) \propto \mathbf{g}_{1N}^+(\mu)$ still holds, and it can be directly numerically checked for finite N that

$\mathbf{g}_{1N}^+(-2\zeta(\alpha)), \mathbf{g}_{1N}^+(2\eta(\alpha)) \sim N^{-1}$, independent of α [57]. This therefore clearly gives the origin of N^{-2} scaling of conductance at $\mu = -2\zeta(\alpha), 2\eta(\alpha)$.

A new type of quantum non-equilibrium phase transition — Since $G(\mu) \propto |\mathbf{G}_{1N}^+(\mu)|^2$, a non-analytic change in $G(\mu)$ corresponds to a non-analytic change in NESS, thereby pointing to a non-equilibrium phase transition. The sub-diffusive to ballistic phase transition is thus a type of non-equilibrium phase transition, that, to our knowledge, has not been discussed before. In existing examples of dissipative phase transitions in the literature that we know of (for example, [63–77]) the phase transition occurs on changing either a parameter in the system Hamiltonian, or the strength of the system-bath couplings. In contrast, here, the phase transition occurs as a function of the chemical potentials of the baths. These are not Hamiltonian parameters, either of the system or of the baths, but rather are the thermodynamic parameters fixed by the initial state of the baths. These control the zero temperature noise that originates from the baths, which, in turn control the NESS.

As is clear from the above results, this phase transition stems from the non-analyticity of the dispersion relation of the system in the thermodynamic limit. It is therefore a property of the system in the large N limit, and is completely independent of details of the baths, as long as there is a unique NESS. In fact to guarantee a unique NESS, only two properties of the bath spectral functions are required: (a) the spectral functions for both the baths must be continuous, (b) the band of the baths must encompass the band of the system. Notably, the strength of system-bath coupling also does not play a role. While it determines the value of conductance, it does not affect the system-size scaling of conductance. This is evident from validity of the conjecture $\mathbf{G}_{1N}^+(\mu) \propto \mathbf{g}_{1N}^+(\mu)$, and can also be verified numerically [57]. However, even though the sub-diffusive behavior emerges from the properties of the system in the thermodynamic limit, the presence of the baths are crucial to allow the chemical potentials to be tuned beyond the system bandwidth. In an isolated system, there would be no contribution of energies outside the system bandwidth in DC transport quantities, like the DC conductivity. Thus, the sub-diffusive behavior observed here has no isolated system analogue.

This phase transition is clearly a quantum phase transition, as it occurs strictly at zero temperature. At any finite temperature, at all values of chemical potentials of the baths, calculation of current or conductance will have finite contribution from energies within the system energy bands. At low temperatures, for chemical potentials outside the system band, this contribution will be small, but as system size is increased, will eventually be the leading contribution. So, at finite but low temperatures, for chemical potentials outside the system band, there will be a crossover from the sub-diffusive to the ballistic behavior as a function of system size. Thus, like

standard quantum phase transitions, this phase transition gives rise to a finite size crossover at finite but low temperatures.

Generality of the sub-diffusive phases— When $\mu < -2\zeta(\alpha)$, it is intuitive and can be numerically checked [57] that there is a sub-extensive number of particles in the system. If a number-conserving interaction term (i.e, higher than quadratic term, for example, $\hat{H}_{\text{int}} = \sum_{\ell,m} V_{\ell m} \hat{c}_{\ell}^{\dagger} \hat{c}_{\ell}^{\dagger} \hat{c}_m^{\dagger} \hat{c}_m$, $\hat{H}_S \rightarrow \hat{H}_S + \hat{H}_{\text{int}}$) is now switched on, at large enough N , due to extremely low particle density in the system, it will play a negligible role for $\mu < -2\zeta(\alpha)$. Similar argument, in terms of holes rather than particles, can be made for $\mu > 2\eta(\alpha)$. Thus, the sub-diffusive phases for chemical potential outside the system band are robust against presence of number-conserving many-body interactions in the system. Therefore, clearly these sub-diffusive phases which have no isolated system analogue are general properties of all number-conserving one-dimensional ordered fermionic systems in presence of long-range hopping decaying as a power-law. But, for $-2\zeta(\alpha) < \mu < 2\eta(\alpha)$, there will be a finite particle density in the system and the interactions can have a non-trivial effect which may change the nature of the transport. Direct demonstration of these statements in presence of many-body interactions is, however, currently beyond the state-of-the-art numerical techniques.

Further remarks and outlook — We have previously remarked that the sub-diffusive scaling of conductance does not depend on the strength of system-bath coupling. However, it is important to note that, the standard second-order weak-coupling Markovian approaches to open systems [78], for example, Born-Markov type quantum master equations in Redfield or Lindblad forms cannot capture these sub-diffusive phases. This is because, in carrying out the Born-Markov approximations, one neglects contributions coming from bath energies which are away from system energy scales. Such an equation would therefore wrongly predict zero conductance for chemical potentials outside the system band at all system sizes.

The results presented here establish a completely new way in which sub-diffusive transport can originate in low-dimensional systems. Our study reveals that transport properties of long-range systems in two terminal open quantum system set-up can be drastically different from both their isolated system and short-ranged system counterparts, featuring new kinds of quantum non-equilibrium phase transitions. Such rich behavior may allow potential applications of long-range systems as novel working media for thermoelectric devices, quantum heat engines and refrigerators [58–60], which will be investigated in future works. The effect of disorder or quasi-periodic potential [54] on open system transport properties of low-dimensional long-range systems also remains to be seen.

Acknowledgement— BKA acknowledges the MATRICS grant MTR/2020/000472 from SERB, Government of India and the Shastri Indo-Canadian Institute for providing financial support for this research work in the form of a Shastri Institutional Collaborative Research Grant (SICRG). MS acknowledge financial support through National Postdoctoral Fellowship (NPDF), SERB file no. PDF/2020/000992. AP acknowledges funding from European Unions Horizon 2020 research and innovation programme under the Marie Skłodowska-Curie grant agreement No. 890884.

* archak.p@tcd.ie

† madhumita.saha@acads.iiserpune.ac.in

‡ bijay@iiserpune.ac.in

- [1] C. G. Smith, *Reports on Progress in Physics* **59**, 235 (1996).
- [2] R. Fleischmann and T. Geisel, *Phys. Rev. Lett.* **89**, 016804 (2002).
- [3] A. M. Zagoskin, Cambridge University Press (2011).
- [4] G. Benenti, G. Casati, K. Saito, and R. S. Whitney, *Physics Reports* **694**, 1 (2017).
- [5] J. J. Palacios, *Nature Physics* **10**, 182 (2014).
- [6] U. Naether, S. Stützer, R. A. Vicencio, M. I. Molina, A. Tünnermann, S. Nolte, T. Kottos, D. N. Christodoulides, and A. Szameit, *New Journal of Physics* **15**, 013045 (2013).
- [7] F. Sgrignuoli and L. Dal Negro, *Phys. Rev. B* **101**, 214204 (2020).
- [8] D. J. Luitz, N. Laflorencie, and F. Alet, *Phys. Rev. B* **93**, 060201 (2016).
- [9] A. C. Potter, R. Vasseur, and S. A. Parameswaran, *Phys. Rev. X* **5**, 031033 (2015).
- [10] K. Agarwal, S. Gopalakrishnan, M. Knap, M. Müller, and E. Demler, *Phys. Rev. Lett.* **114**, 160401 (2015).
- [11] R. Vosk, D. A. Huse, and E. Altman, *Phys. Rev. X* **5**, 031032 (2015).
- [12] W. De Roeck, F. Huveneers, and S. Olla, *Journal of Statistical Physics* **180**, 678 (2020).
- [13] S. R. Taylor and A. Scardicchio, (2021), [arXiv:2007.13783](https://arxiv.org/abs/2007.13783) [cond-mat.dis-nn].
- [14] A. Purkayastha, S. Sanyal, A. Dhar, and M. Kulkarni, *Phys. Rev. B* **97**, 174206 (2018).
- [15] A. Purkayastha, A. Dhar, and M. Kulkarni, *Phys. Rev. B* **96**, 180204 (2017).
- [16] A. Purkayastha, *Journal of Statistical Mechanics: Theory and Experiment* **2019**, 043101 (2019).
- [17] J. Sutradhar, S. Mukerjee, R. Pandit, and S. Banerjee, *Phys. Rev. B* **99**, 224204 (2019).
- [18] H. Hiramoto and S. Abe, *Journal of the Physical Society of Japan* **57**, 230 (1988).
- [19] J. Zhong, R. B. Diener, D. A. Steck, W. H. Oskay, M. G. Raizen, E. W. Plummer, Z. Zhang, and Q. Niu, *Phys. Rev. Lett.* **86**, 2485 (2001).
- [20] A. Jagannathan, (2021), [arXiv:2012.14744](https://arxiv.org/abs/2012.14744) [cond-mat.stat-mech].
- [21] M. Kohmoto, B. Sutherland, and C. Tang, *Phys. Rev. B* **35**, 1020 (1987).
- [22] J. X. Zhong and R. Mosseri, *Journal of Physics: Con-*

- densed Matter **7**, 8383 (1995).
- [23] J. Settimo, N. W. Talarico, F. Cosco, F. Plastina, S. Maniscalco, and N. Lo Gullo, *Phys. Rev. B* **101**, 144303 (2020).
 - [24] Y. B. Lev, D. M. Kennes, C. Klöckner, D. R. Reichman, and C. Karrasch, *EPL (Europhysics Letters)* **119**, 37003 (2017).
 - [25] V. K. Varma and M. Žnidarič, *Phys. Rev. B* **100**, 085105 (2019).
 - [26] C. Chiaracane, F. Pietracaprina, A. Purkayastha, and J. Goold, (2021), [arXiv:2101.01111 \[cond-mat.dis-nn\]](https://arxiv.org/abs/2101.01111).
 - [27] M. Saha, A. Purkayastha, and S. K. Maiti, *Journal of Physics: Condensed Matter* **32**, 025303 (2019).
 - [28] I. I. Ryabtsev, D. B. Tretyakov, I. I. Beterov, and V. M. Entin, *Phys. Rev. Lett.* **104**, 073003 (2010).
 - [29] L. Béguin, A. Vernier, R. Chicireanu, T. Lahaye, and A. Browaeys, *Phys. Rev. Lett.* **110**, 263201 (2013).
 - [30] A. Browaeys, D. Barredo, and T. Lahaye, *Journal of Physics B: Atomic, Molecular and Optical Physics* **49**, 152001 (2016).
 - [31] S. Korenblit, D. Kafri, W. C. Campbell, R. Islam, E. E. Edwards, Z.-X. Gong, G.-D. Lin, L.-M. Duan, J. Kim, K. Kim, and C. Monroe, *New Journal of Physics* **14**, 095024 (2012).
 - [32] P. Jurcevic, H. Shen, P. Hauke, C. Maier, T. Brydges, C. Hempel, B. P. Lanyon, M. Heyl, R. Blatt, and C. F. Roos, *Phys. Rev. Lett.* **119**, 080501 (2017).
 - [33] B. Neyenhuis, J. Zhang, P. W. Hess, J. Smith, A. C. Lee, P. Richerme, Z.-X. Gong, A. V. Gorshkov, and C. Monroe, *Science Advances* **3** (2017), [10.1126/sciadv.1700672](https://doi.org/10.1126/sciadv.1700672).
 - [34] J. W. Britton, B. C. Sawyer, A. C. Keith, C. C. J. Wang, J. K. Freericks, H. Uys, M. J. Biercuk, and J. J. Bollinger, *Nature* **484**, 489 EP (2012).
 - [35] P. Richerme, Z.-X. Gong, A. Lee, C. Senko, J. Smith, M. Foss-Feig, S. Michalakakis, A. V. Gorshkov, and C. Monroe, *Nature* **511**, 198 EP (2014).
 - [36] P. Jurcevic, B. P. Lanyon, P. Hauke, C. Hempel, P. Zoller, R. Blatt, and C. F. Roos, *Nature* **511**, 202 EP (2014).
 - [37] J. Zhang, G. Pagano, P. W. Hess, A. Kyprianidis, P. Becker, H. Kaplan, A. V. Gorshkov, Z.-X. Gong, and C. Monroe, *Nature* **551**, 601 EP (2017).
 - [38] J. Zhang, P. W. Hess, A. Kyprianidis, P. Becker, A. Lee, J. Smith, G. Pagano, I.-D. Potirniche, A. C. Potter, A. Vishwanath, N. Y. Yao, and C. Monroe, *Nature* **543**, 217 EP (2017).
 - [39] C. Maier, T. Brydges, P. Jurcevic, N. Trautmann, C. Hempel, B. P. Lanyon, P. Hauke, R. Blatt, and C. F. Roos, *Phys. Rev. Lett.* **122**, 050501 (2019).
 - [40] B. Yan, S. A. Moses, B. Gadway, J. P. Covey, K. R. A. Hazzard, A. M. Rey, D. S. Jin, and J. Ye, *Nature* **501**, 521 EP (2013).
 - [41] K.-K. Ni, S. Ospelkaus, M. H. G. de Miranda, A. Pe'er, B. Neyenhuis, J. J. Zirbel, S. Kotochigova, P. S. Julienne, D. S. Jin, and J. Ye, *Science* **322**, 231 (2008).
 - [42] S. A. Moses, J. P. Covey, M. T. Miecnikowski, D. S. Jin, and J. Ye, *Nature Physics* **13**, 13 EP (2016).
 - [43] A. de Paz, A. Sharma, A. Chotia, E. Maréchal, J. H. Huckans, P. Pedri, L. Santos, O. Gorceix, L. Vernac, and B. Laburthe-Tolra, *Phys. Rev. Lett.* **111**, 185305 (2013).
 - [44] G. A. Álvarez, D. Suter, and R. Kaiser, *Science* **349**, 846 (2015).
 - [45] S. Choi, J. Choi, R. Landig, G. Kucsko, H. Zhou, J. Isoya, F. Jelezko, S. Onoda, H. Sumiya, V. Khemani, C. von Keyserlingk, N. Y. Yao, E. Demler, and M. D. Lukin, *Nature* **543**, 221 EP (2017).
 - [46] S. Smale, P. He, B. A. Olsen, K. G. Jackson, H. Sharum, S. Trotzky, J. Marino, A. M. Rey, and J. H. Thywissen, *Science Advances* **5** (2019).
 - [47] M. Saha, S. K. Maiti, and A. Purkayastha, *Phys. Rev. B* **100**, 174201 (2019).
 - [48] S. Akhanejee, *Phys. Rev. B* **79**, 205101 (2009).
 - [49] B. Kloss and Y. Bar Lev, *Phys. Rev. A* **99**, 032114 (2019).
 - [50] B. Kloss and Y. Bar Lev, *Phys. Rev. B* **102**, 060201 (2020).
 - [51] K. Kawa and P. Machnikowski, *Phys. Rev. B* **102**, 174203 (2020).
 - [52] J. T. Schneider, J. Despres, S. J. Thomson, L. Tagliacozzo, and L. Sanchez-Palencia, *Phys. Rev. Research* **3**, L012022 (2021).
 - [53] Y. Prasad and A. Garg, *Phys. Rev. B* **103**, 064203 (2021).
 - [54] R. Modak and T. Nag, *Phys. Rev. Research* **2**, 012074 (2020).
 - [55] M. Katzer, W. Knorr, R. Finsterhölzl, and A. Carmele, *Phys. Rev. B* **102**, 125101 (2020).
 - [56] M. M. Roses, H. Landa, and E. G. D. Torre, (2021), [arXiv:2102.09590 \[quant-ph\]](https://arxiv.org/abs/2102.09590).
 - [57] See supplemental material.
 - [58] R. Kosloff and A. Levy, *Annual Review of Physical Chemistry* **65**, 365 (2014), PMID: 24689798.
 - [59] G. Benenti, G. Casati, K. Saito, and R. S. Whitney, *Physics Reports* **694**, 1 (2017).
 - [60] G. T. Landi, D. Poletti, and G. Schaller, “Non-equilibrium boundary driven quantum systems: models, methods and properties,” (2021), [arXiv:2104.14350 \[quant-ph\]](https://arxiv.org/abs/2104.14350).
 - [61] H. Haug and A.-P. Jauho, *Quantum Kinetics in Transport and Optics of Semiconductors* (Springer-Verlag Berlin Heidelberg, 2008).
 - [62] M. Di Ventra, *Electrical Transport in Nanoscale Systems* (Cambridge University Press, 2008).
 - [63] S. R. K. Rodriguez, W. Casteels, F. Storme, N. Carlon Zambon, I. Sagnes, L. Le Gratiet, E. Galopin, A. Lemaître, A. Amo, C. Ciuti, and J. Bloch, *Phys. Rev. Lett.* **118**, 247402 (2017).
 - [64] T. L. Heugel, M. Biondi, O. Zilberberg, and R. Chitra, *Phys. Rev. Lett.* **123**, 173601 (2019).
 - [65] J. M. Fink, A. Dombi, A. Vukics, A. Wallraff, and P. Domokos, *Phys. Rev. X* **7**, 011012 (2017).
 - [66] M. Fitzpatrick, N. M. Sundaresan, A. C. Y. Li, J. Koch, and A. A. Houck, *Phys. Rev. X* **7**, 011016 (2017).
 - [67] M. Jo, J. Lee, K. Choi, and B. Kahng, *Phys. Rev. Research* **3**, 013238 (2021).
 - [68] O. Gamayun, A. Slobodeniuk, J.-S. Caux, and O. Lychkovskiy, *Phys. Rev. B* **103**, L041405 (2021).
 - [69] A. Zamora, G. Dagvadorj, P. Comaron, I. Carusotto, N. P. Proukakis, and M. H. Szymańska, *Phys. Rev. Lett.* **125**, 095301 (2020).
 - [70] M. Jo, J. Um, and B. Kahng, *Phys. Rev. E* **99**, 032131 (2019).
 - [71] F. Carollo, E. Gillman, H. Weimer, and I. Lesanovsky, *Phys. Rev. Lett.* **123**, 100604 (2019).
 - [72] F. Minganti, A. Biella, N. Bartolo, and C. Ciuti, *Phys. Rev. A* **98**, 042118 (2018).
 - [73] M. Marcuzzi, M. Buchhold, S. Diehl, and I. Lesanovsky, *Phys. Rev. Lett.* **116**, 245701 (2016).
 - [74] G. Dagvadorj, J. M. Fellows, S. Matyjaśkiewicz, F. M. Marchetti, I. Carusotto, and M. H. Szymańska, *Phys.*

- Rev. X **5**, 041028 (2015).
- [75] D. Nagy and P. Domokos, *Phys. Rev. Lett.* **115**, 043601 (2015).
- [76] V. M. Bastidas, C. Emary, B. Regler, and T. Brandes, *Phys. Rev. Lett.* **108**, 043003 (2012).
- [77] T. Prosen and I. Pizorn, *Phys. Rev. Lett.* **101**, 105701 (2008).
- [78] H.-P. Breuer and F. Petruccione, *The Theory of Open Quantum Systems* (Oxford University Press, 2007).

Supplemental Material: Sub-diffusive phases in open clean long-range systems

Archak Purkayastha,^{1,*} Madhumita Saha,^{2,†} and Bijay Kumar Agarwalla^{2,‡}

¹*Department of Physics, Trinity College Dublin, Dublin, Ireland*

²*Department of Physics, Indian Institute of Science Education and Research Pune,
Dr. Homi Bhabha Road, Ward No. 8, NCL Colony, Pashan, Pune, Maharashtra 411008, India*
(Dated: April 26, 2022)

S1. EXACT ANALYTICAL DISPERSION RELATION FOR ISOLATED SYSTEM IN THE THERMODYNAMIC LIMIT

In the derivation of our main results, we have used the bare Green's function of the isolated system in the thermodynamic limit. In this section we derive the dispersion relation for the clean long-range isolated system. First, we take our system Hamiltonian in Eq.(7) and re-label the sites to $r \rightarrow r - \frac{N}{2} - 1$, assuming, for simplicity, that N is even,

$$\hat{\mathcal{H}}_S = - \sum_{m=1}^N \left(\sum_{r=-N/2}^{N/2-1-m} \frac{1}{m^\alpha} \left(\hat{c}_r^\dagger \hat{c}_{r+m} + \hat{c}_{r+m}^\dagger \hat{c}_r \right) \right). \quad (\text{S1})$$

Next, we take $N \rightarrow \infty$ in the above equation. This gives,

$$\hat{\mathcal{H}}_S = - \sum_{r=-\infty}^{\infty} \sum_{m=1}^{\infty} \frac{1}{m^\alpha} \left(\hat{c}_r^\dagger \hat{c}_{r+m} + \hat{c}_{r+m}^\dagger \hat{c}_r \right), \quad (\text{S2})$$

where we have neglected some boundary terms. Now the system has translational invariance. We can diagonalize the above Hamiltonian by going to momentum space via a Fourier transform,

$$\begin{aligned} \hat{c}(k) &= \sum_{r=-\infty}^{\infty} \hat{c}_r e^{irk}, \quad k \in [-\pi, \pi] \\ \hat{c}_r &= \frac{1}{2\pi} \int_{-\pi}^{\pi} dk e^{-irk} \hat{c}(k). \end{aligned} \quad (\text{S3})$$

This gives

$$\hat{\mathcal{H}}_S = \int_{-\pi}^{\pi} dk \varepsilon(k, \alpha) \hat{c}^\dagger(k) \hat{c}(k), \quad (\text{S4})$$

with the dispersion relation

$$\varepsilon(k, \alpha) = -2 \sum_{m=1}^{\infty} \frac{\cos(mk)}{m^\alpha}. \quad (\text{S5})$$

The Green's function of the isolated system in the thermodynamic limit in the momentum-frequency space is then given by

$$g(k, \omega) = \lim_{\epsilon \rightarrow 0} \frac{1}{\omega - \varepsilon(k, \alpha) - i\epsilon}. \quad (\text{S6})$$

Returning to the site basis ($p, q = \{1, N\}$), we get the bare Green's function as

$$\mathbf{g}_{pq}(\omega) = \lim_{\epsilon \rightarrow 0} \frac{1}{2\pi} \int_{-\pi}^{\pi} dk \frac{e^{-ik|p-q|}}{\omega - \varepsilon(k, \alpha) - i\epsilon}. \quad (\text{S7})$$

* archak.p@tcd.ie

† madhumita.saha@acads.iiserpune.ac.in

‡ bijay@iiserpune.ac.in

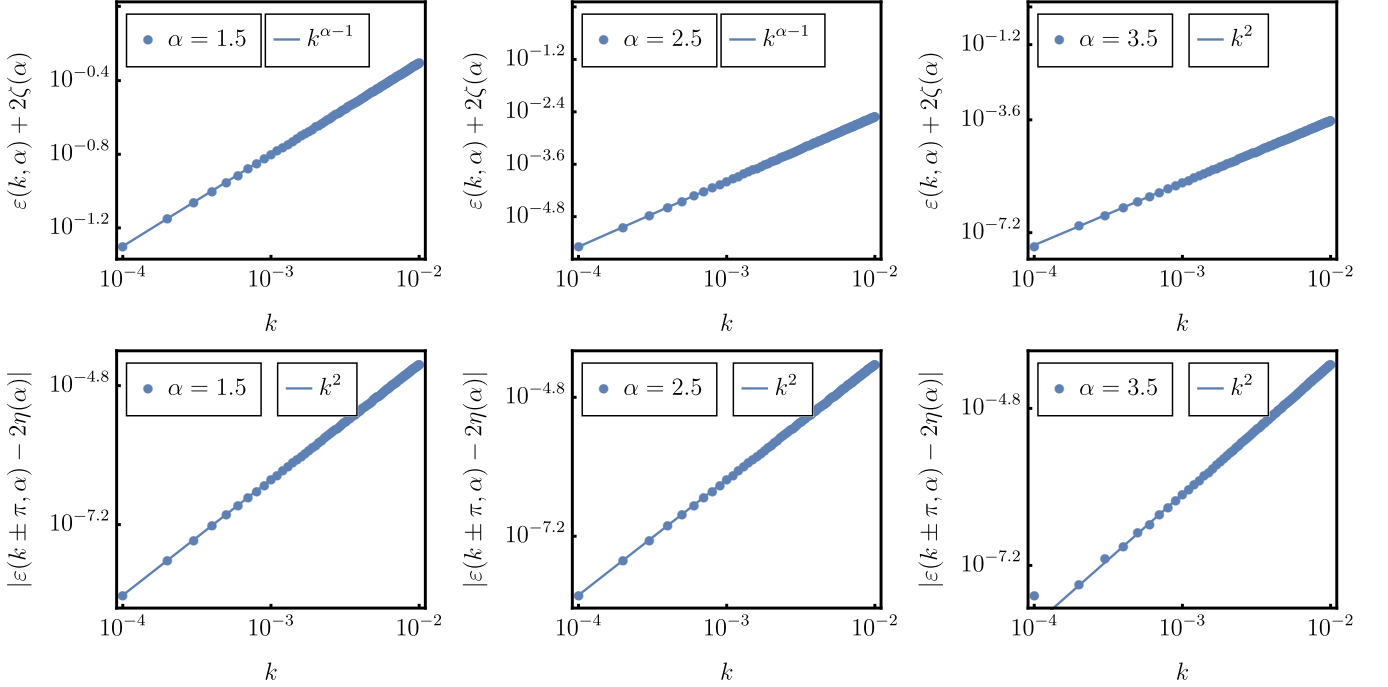


FIG. S1. (Color online) In the first row, numerically we have plotted $\varepsilon(k, \alpha) + 2\zeta(\alpha)$ in small k regime for $\alpha = 1.5, 2.5$ and 3.5 respectively. For $\alpha < 3$, $\varepsilon(k, \alpha) + 2\zeta(\alpha) \sim k^{\alpha-1}$ and for $\alpha > 3$, $\varepsilon(k, \alpha) + 2\zeta(\alpha) \sim k^2$. This also matches with our analytical result eq. S16. Similarly, in the second row, we have plotted $|\varepsilon(k \pm \pi, \alpha) - 2\eta(\alpha)|$ in small k regime for three different values of α . Here we can see $|\varepsilon(k \pm \pi, \alpha) - 2\eta(\alpha)|$ always goes as k^2 . This also matches with our analytical result eq. S18.

S2. PROPERTIES OF THE DISPERSION RELATION

In this section, we state the relevant properties of the dispersion relation which are crucial for the proof of the scaling in conductance. The infinite series giving the dispersion relation is absolutely convergent for all k when $\alpha > 1$. The following relation holds connecting $\varepsilon(k, \alpha)$ with $\varepsilon(k \pm \pi, \alpha) = 2 \sum_{m=1}^{\infty} (-1)^{m-1} \frac{\cos(mk)}{m^\alpha}$,

$$\varepsilon(k \pm \pi, \alpha) = -\varepsilon(k, \alpha) + 2^{1-\alpha} \varepsilon(2k, \alpha) \quad (\text{S8})$$

The minimum of the dispersion relation is given at $k = 0$,

$$\varepsilon_{\min}(\alpha) = \varepsilon(0, \alpha) = -2\zeta(\alpha), \quad (\text{S9})$$

where $\zeta(\alpha) = \sum_{m=1}^{\infty} \frac{1}{m^\alpha}$ is the Reimann-zeta function. Similarly, the maximum of the dispersion relation is at $k = \pm\pi$,

$$\varepsilon_{\max}(\alpha) = \varepsilon(\pm\pi, \alpha) = 2\eta(\alpha), \quad (\text{S10})$$

where $\eta(\alpha)$ is the Dirichlet eta function, $\eta(\alpha) = \sum_{m=1}^{\infty} \frac{(-1)^{m-1}}{m^\alpha} = (1 - 2^{1-\alpha})\zeta(\alpha)$, also known as the alternating zeta function. Importantly, the dispersion relation is non-analytic at $k = 0$ for all values of α . This is because,

$$\lim_{k \rightarrow 0} \frac{\partial^p \varepsilon(k, \alpha)}{\partial k^p} \rightarrow \infty, \quad \forall p > \alpha - 1. \quad (\text{S11})$$

Thus a Taylor expansion around $k = 0$ does not exist. However, we still need to find the small k behavior of $\varepsilon(k, \alpha)$. To do this we define

$$f(sk, \alpha) = \zeta(\alpha) + \frac{\varepsilon(sk, \alpha)}{2} = \sum_{m=1}^{\infty} \frac{1 - \cos(sm)}{m^\alpha}. \quad (\text{S12})$$

Here, s is an integer. Next, we divide the summation in the right-hand-side into two parts,

$$\begin{aligned} f(sk, \alpha) &= \sum_{m=1}^{1/s|k|} \frac{1 - \cos(sm k)}{m^\alpha} + |k|^\alpha B, \\ B &= \sum_{y \geq 1/s} \frac{1 - \cos(sy)}{y^\alpha} \simeq s^{\alpha-1} \int_1^\infty dy' \frac{1 - \cos(y')}{y'^\alpha} \\ &\simeq s^{\alpha-1} B', \quad B' = \int_1^\infty dy' \frac{1 - \cos(y')}{y'^\alpha} \end{aligned}$$

where we have used $y = m|k|$ and $y' = sy$. The expression in the definition of B' converges. Thus B' is a real number which depends on α . Now we expand the cosine to obtain

$$f(sk, \alpha) = s^{\alpha-1} |k|^\alpha B' - \sum_{p=1}^\infty \frac{(-1)^p s^{2p} k^{2p}}{(2p)!} \sum_{m=1}^{1/s|k|} \frac{1}{m^{\alpha-2p}}. \quad (\text{S13})$$

Till now, the expression is exact. After this we make some approximations and assumptions. We replace the summation over m by an integration and further assume that α is not an integer. This then gives,

$$\begin{aligned} f(sk, \alpha) &\simeq s^{\alpha-1} |k|^\alpha B' - \sum_{p=1}^\infty \frac{(-1)^p s^{2p} k^{2p}}{(2p)!} \frac{(1/s|k|)^{2p-\alpha+1} - 1}{2p - \alpha + 1} \\ &= s^{\alpha-1} |k|^\alpha B' + s^{\alpha-1} |k|^{\alpha-1} a_1 - \sum_{p=1}^\infty \frac{(-1)^{p+1} s^{2p} k^{2p}}{(2p)! (2p - \alpha + 1)}, \\ a_1 &= \sum_{p=1}^\infty \frac{(-1)^{p+1}}{(2p)! (2p - \alpha + 1)}, \quad \alpha > 1, \alpha \notin \mathbb{Z}, \end{aligned} \quad (\text{S14})$$

where \mathbb{Z} is the set of all integers. It can be checked by ratio test that the infinite series in the definition of a_1 converges. So, a_1 is a real number which depends on α . Now considering $s = 1$, we have an approximate series expansion for $\varepsilon(k, \alpha)$ around $k = 0$,

$$\begin{aligned} \varepsilon(k, \alpha) &\simeq -2 \left[\zeta(\alpha) - |k|^{\alpha-1} a_1 - |k|^\alpha B' \right. \\ &\quad \left. + \sum_{p=1}^\infty \frac{(-1)^{p+1} k^{2p}}{(2p)! (2p - \alpha + 1)} \right] \end{aligned} \quad (\text{S15})$$

It is interesting to note that a_1 , which is the coefficient of $|k|^{\alpha-1}$, has contribution from all terms coming from the expansion of the cosine. This is consistent with the fact that Taylor series expansion around $k = 0$ is invalid. The presence of absolute values and the terms raised to non-integer powers, both of which make $k = 0$ non-analytic, clearly distinguishing the above series expansion from a Taylor series expansion. Armed with the series expansion, we obtain the small k behavior of the dispersion relation by keeping the lowest order terms with non-integer and integer powers,

$$\begin{aligned} \varepsilon(k, \alpha) &\simeq -2 \left[\zeta(\alpha) - a_1 |k|^{\alpha-1} - a_2 k^2 \right], \quad |k| \ll 1, \\ a_2 &= \frac{1}{2(\alpha - 3)}. \end{aligned} \quad (\text{S16})$$

Similarly putting $s = 2$ in Eq.(S14) one can compute,

$$\begin{aligned} \varepsilon(2k, \alpha) &\simeq -2 \left[\zeta(\alpha) - 2^{\alpha-1} |k|^{\alpha-1} a_1 - 2^{\alpha-1} |k|^\alpha B' \right. \\ &\quad \left. + \sum_{p=1}^\infty \frac{(-1)^{p+1} 2^{2p} k^{2p}}{(2p)! (2p - \alpha + 1)} \right] \end{aligned} \quad (\text{S17})$$

Further, using Eq.(S15) and Eq.(S17) in Eq.(S8) and considering the leading order term $p = 1$ we can also obtain an equivalent expansion around $k = \pm\pi$,

$$\begin{aligned} \varepsilon(k \pm \pi, \alpha) &\simeq 2 \eta(\alpha) - 2a_2(1 - 2^{3-\alpha})k^2, \\ |k| &\ll 1. \end{aligned} \quad (\text{S18})$$

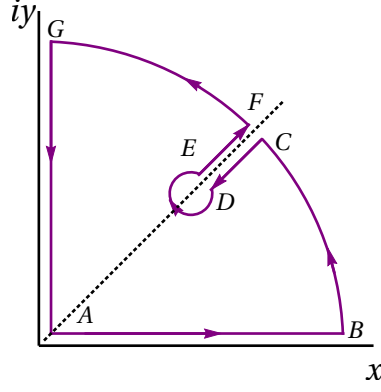


FIG. S2. The contour chosen to carry out the integration in Eq.(S23).

which is analytic as the expansion contains only integer powers. The above two expansions are used to obtain the scaling of current with system size. We have also checked this two expansions eq. S16 and eq. S18 numerically in fig.S1. Though the above expansions are obtained for non-integer values of α , the results can be analytically continued to include integer values of $\alpha > 1$ by making the fractional part arbitrarily small.

S3. ANALYTICAL SCALING OF $\mathbf{G}_{1N}^+(\mu)$ WITH SYSTEM SIZE

Our main conjecture is that for large N the system size scaling of $\mathbf{G}_{1N}^+(\mu)$ will be same as that of the bare Green's function $\mathbf{g}_{1N}^+(\mu)$, i.e, $\mathbf{G}_{1N}^+(\mu) \propto \mathbf{g}_{1N}(\mu)$, with proportionality constant being independent of N . If we further assume that $\mathbf{g}_{1N}^+(\mu)$ is evaluated in the thermodynamic limit, we get

$$\mathbf{G}_{1N}^+(\mu) \sim \lim_{\epsilon \rightarrow 0} \frac{1}{2\pi} \int_{-\pi}^{\pi} dk \frac{e^{-ikN}}{\mu - \varepsilon(k, \alpha) - i\epsilon} = \mathcal{G}_{1N}^+(\mu). \quad (\text{S19})$$

The major contribution to the integral on the right-hand-side comes from the singularities of the integrand.

Case 1: $-2\zeta(\alpha) < \mu < 2\eta(\alpha)$: Clearly, if μ lies within the bandwidth of the system, $-2\zeta(\alpha) < \mu < 2\eta(\alpha)$, then the integrand will have poles on the real line. Poles on the real line can, at best, generate terms which oscillate with N , and not any scaling behavior with N . So, as far as system size scaling is concerned, we can infer,

$$\mathbf{G}_{1N}^+(\mu) \sim N^0 \quad \forall \quad -2\zeta(\alpha) < \mu < 2\eta(\alpha). \quad (\text{S20})$$

This is what leads to the ballistic behavior of current.

Case 2: $\mu < -2\zeta(\alpha)$: Next, we consider the case when μ lies below the lower band edge i.e., $\mu \leq -2\zeta(\alpha)$ which is our main regime of interest. In this case, the maximum contribution to the integral comes from small values of k . Therefore we use Eq.(S16) to obtain

$$\begin{aligned} \frac{1}{\mu - \varepsilon(k, \alpha) - i\epsilon} &\simeq -\frac{1}{a_0(\omega) + 2a_1|k|^{\alpha-1} + 2a_2k^2 + i\epsilon}, \\ a_0(\mu) &= -2\zeta(\alpha) - \mu \geq 0. \end{aligned} \quad (\text{S21})$$

Then we have,

$$\mathbf{G}_{1N}^+(\mu) \sim -\frac{1}{2\pi} \int_{-\infty}^{\infty} dk \frac{e^{-ikN}}{a_0(\mu) + 2a_1|k|^{\alpha-1} + 2a_2k^2 + i\epsilon} = -\frac{1}{2\pi} (A_+ + A_-), \quad (\text{S22})$$

where we have extended both the upper and the lower limit of the integral to infinity since we have already assumed that large values of k gives a negligible contribution. Here

$$A_{\pm} = \int_0^{\infty} dk \frac{e^{\mp ikN}}{a_0(\mu) + 2a_1|k|^{\alpha-1} + 2a_2k^2 + i\epsilon} \quad (\text{S23})$$

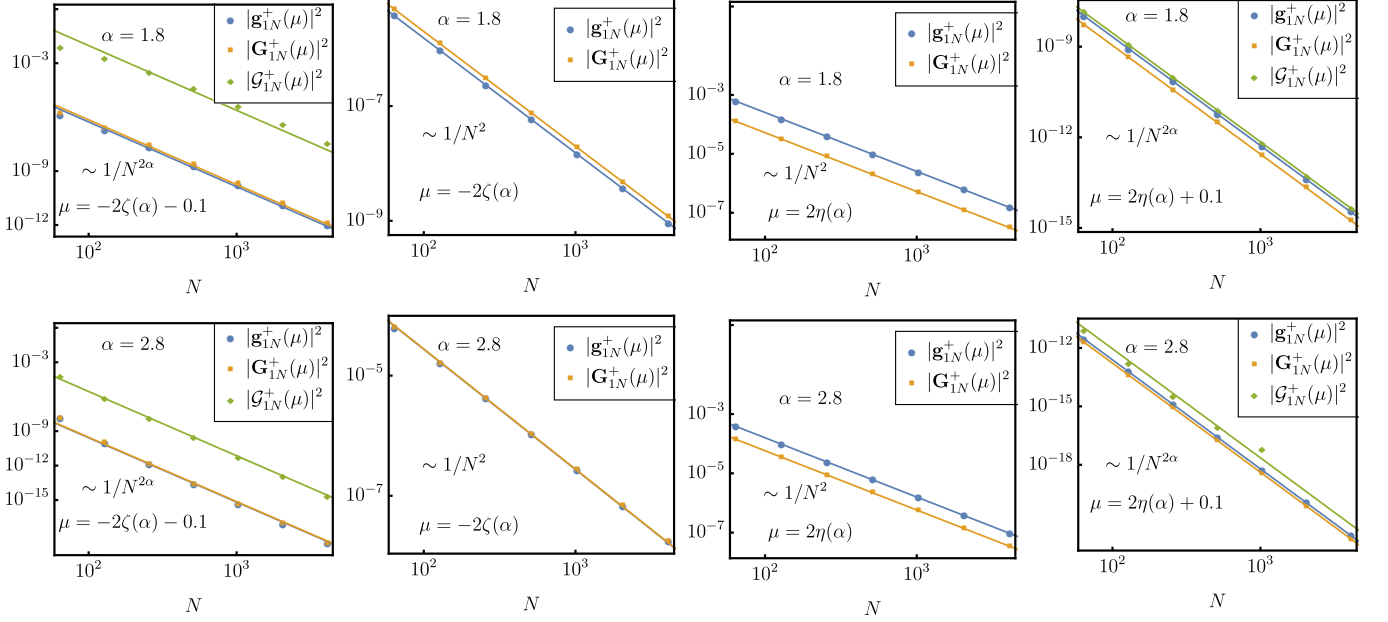


FIG. S3. (Color online). Here numerically we have shown system size scaling of three different Green's functions (i) central system's bare Green's function $\mathbf{g}_{1N}^+(\mu)$, (ii) actual Green's function $\mathbf{G}_{1N}^+(\mu)$ that appears in the conductance formula (iii) further approximated bare Green's function $\mathcal{G}_{1N}^+(\mu)$. The first row is for $\alpha = 1.8$ and the second row is for $\alpha = 2.8$. For the calculation of $\mathbf{G}_{1N}^+(\mu)$, the bath spectral functions are chosen to be $\mathfrak{J}_1(\omega) = \mathfrak{J}_N(\omega) = \Gamma \sqrt{1 - (\frac{\omega}{\Lambda})^2}$, with $\Lambda = 10$ and $\Gamma = 1.6$. We can see that all the Green's functions can capture the $1/N^{2\alpha}$ scaling outside the band edge for both $\alpha = 1.8$ and 2.8 . At the edges $1/N^2$ scaling can not be captured by $\mathcal{G}_{1N}^+(\mu)$ but it is captured by systems's bare Green's function $\mathbf{g}_{1N}^+(\mu)$. It also ensures that all these sub-diffusive scalings are actually the property of the central system.

The integration in Eq.(S23) can be carried out using contour integration techniques, by choosing a proper contour as shown in Fig.(S2). This is a valid contour for computing A_- , whereas for A_+ a valid contour is the one enclosing the lower half of the complex plane. Let us first focus on computing A_- . Depending on the value of α , the integrand may or may not have branch point singularities in the right upper half plane. In Fig.(S2), we assume there is one such singularity. For $\alpha > 3$, it can be argued that this will be case, since the $k^{\alpha-1}$ term in the denominator will be sub-leading. By carrying out the integration along the curves CD, DE and EF in the contour, it can be checked that the contribution from them scales with system size as e^{-aN} , ($a > 0$). So, the contribution from any branch point singularity in the right upper half plane is exponentially decaying with system size. The contribution from BC and FG is zero, as is standard. The leading contribution then comes from the line GA of the contour. The integral along the line GA, after some simplification is

$$A_-|_{\text{GA}} = \frac{i}{N} \int_0^\infty dy \frac{e^{-y}}{x_R + ix_I}, \quad A_+|_{\text{GA}} = -\frac{i}{N} \int_0^\infty dy \frac{e^{-y}}{x_R + i\tilde{x}_I}, \quad (\text{S24})$$

where

$$\begin{aligned} x_R &= a_0 + 2a_1 \left(\frac{y}{N}\right)^{\alpha-1} \cos \left[\frac{\pi(\alpha-1)}{2}\right] - 2a_2 \left(\frac{y}{N}\right)^2, \\ x_I &= \epsilon + 2a_1 \left(\frac{y}{N}\right)^{\alpha-1} \sin \left[\frac{\pi(\alpha-1)}{2}\right], \\ \tilde{x}_I &= \epsilon - 2a_1 \left(\frac{y}{N}\right)^{\alpha-1} \sin \left[\frac{\pi(\alpha-1)}{2}\right], \end{aligned} \quad (\text{S25})$$

One can finally write

$$\mathbf{G}_{1N}^+(\mu) \sim -\frac{2a_1 \sin \left[\frac{\pi(\alpha-1)}{2}\right]}{N^\alpha \pi} \int_0^\infty dy \frac{e^{-y} y^{\alpha-1}}{(x_R + ix_I)(x_R + i\tilde{x}_I)} \quad (\text{S26})$$

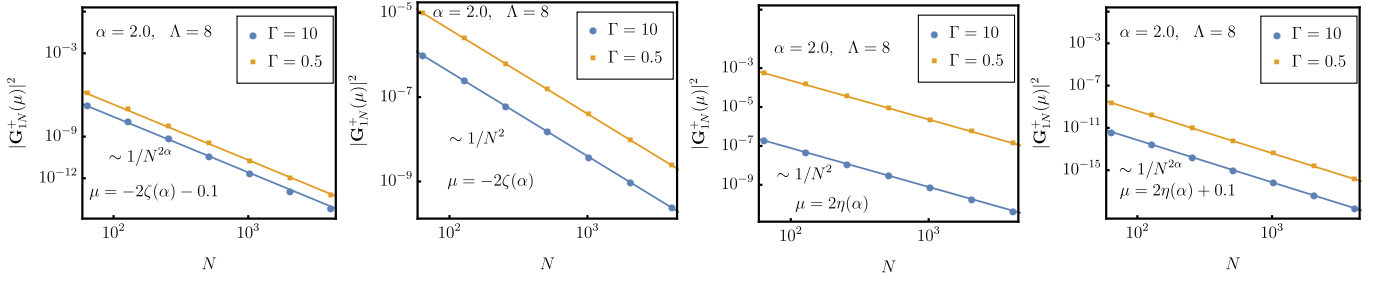


FIG. S4. (Color online). We have plotted the system size scaling of exact Green's function $\mathbf{G}_{1N}^+(\mu)$ for different system-bath couplings for $\alpha = 2$. Here, we can see all the scaling properties are unaffected by the strength of system-bath coupling. For the plots, the bath spectral functions are chosen to be $\mathfrak{J}_1(\omega) = \mathfrak{J}_N(\omega) = \Gamma\sqrt{1 - (\frac{\omega}{\Lambda})^2}$, with $\Lambda = 8$.

Given that a_0 is finite, one can ignore N dependent terms in x_R, x_I, \tilde{x}_I in the thermodynamics limit ($N \rightarrow \infty$) leading to $1/N^\alpha$ dependence for the NEGF and thus conductance $G(\mu)$ scaling as $\sim N^{-2\alpha}$.

Case 3: $\mu > 2\eta(\alpha)$: A similar analysis like above can be done also in the case when μ lies above the maximum band energy $2\eta(\alpha)$ corresponding to $k = \pm\pi$. Interestingly, as $\varepsilon(k \pm \pi)$ is analytic around $k = \pm\pi$, (Eq. (S18)), it is easy to show that this leads to an exponential contribution in the system size, i.e., $\mathbf{G}_{1N}^+(\mu) \sim e^{-bN}$, $b > 0$. The leading order contribution in N once again arises from the non-analyticity behavior of the dispersion relation at $k = 0$ and following similar contour integration steps as above one obtains exactly the same scaling

$$\mathbf{G}_{1N}^+(\mu) \sim N^{-\alpha}, \quad \forall \mu < -2\zeta(\alpha), \mu > 2\eta(\alpha) \quad (\text{S27})$$

Case 4: $\mu = 2\eta(\alpha)$, and $\mu = -2\zeta(\alpha)$: At any finite N , these values of μ do not correspond to any eigenvalue of \mathbf{H} , but the minimum and the maximum eigenvalues of \mathbf{H} tend to these values with increase in N . We find that this case is difficult to obtain from scaling of $\mathcal{G}_{1N}(\omega)$ defined in Eq.(S19). In other words, we cannot use the expression for $\mathbf{g}_{1N}(\mu)$ in the thermodynamic limit. However, direct numerical evaluation gives $\mathbf{G}_{1N}^+(\mu) \propto \mathbf{g}_{1N}(\mu)$, confirming the original conjecture, as we show in the next section.

S4. NUMERICAL SCALING OF $\mathbf{g}_{1N}^+(\mu), \mathbf{G}_{1N}^+(\mu), \mathcal{G}_{1N}^+(\mu)$ WITH SYSTEM SIZE

In the previous section, we have analytically calculated the approximated bare Green's function $\mathcal{G}_{1N}^+(\mu)$ for different cases like inside the band and outside the band. The analytical results give clear understanding of sub-diffusive behaviour ($1/N^{2\alpha}$) outside the band and ballistic behaviour N^0 inside the band. But, this approximated Green's function $\mathcal{G}_{1N}^+(\mu)$ can not capture the sub-diffusive scaling $1/N^2$ at the two band edges. Thus, numerically we have plotted system size scaling of all three different Green's functions (i) central system's bare Green's function $\mathbf{g}_{1N}^+(\mu)$, (ii) actual Green's function $\mathbf{G}_{1N}^+(\mu)$ that appears in the conductance formula (iii) approximated bare Green's function $\mathcal{G}_{1N}^+(\mu)$ in Fig. S3 for $\alpha = 1.8$ and $\alpha = 2.8$. Here, we can numerically also see that all the Green's function can capture the sub-diffusive scaling ($1/N^{2\alpha}$) outside the band. The scaling at band-edge can not be captured by $\mathcal{G}_{1N}^+(\mu)$ but can be captured by system's bare Green's function $\mathbf{g}_{1N}^+(\mu)$.

S5. EFFECT OF SYSTEM-BATH COUPLING

In the main text, we have said that the system-size scaling of conductance is independent of the strength of system-bath coupling. In this section, we explicitly check this numerically. In Fig. S4, we have shown the system size scaling of $\mathbf{G}_{1N}^+(\mu)$ for two widely different strengths of system-bath coupling. We clearly see that all the scaling properties are unaffected by the system-bath coupling strength.

S6. PARTICLE DENSITY IN THE SYSTEM

In the main text, we have remarked that there is a sub-extensive number of particle in the system for $\mu < -2\zeta(\alpha)$, while there is a sub-extensive number of holes for $\mu > 2\eta(\alpha)$. For $-2\zeta(\alpha) < \mu < 2\eta(\alpha)$, there is an extensive number

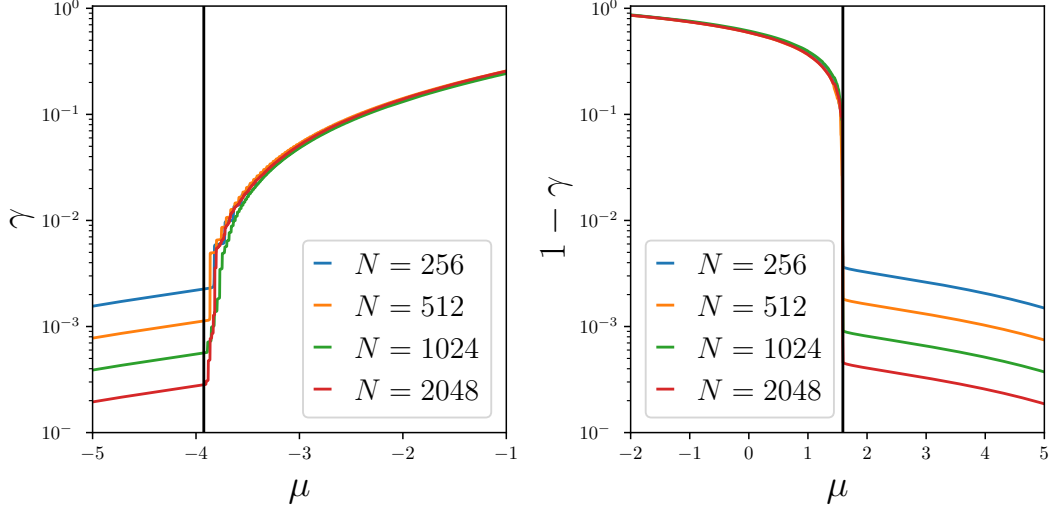


FIG. S5. **(a)** The particle density γ in the system is plotted as a function of chemical potential at zero temperature. The vertical black line corresponds to $\mu = -2\zeta(\alpha)$. For $\mu < -2\zeta(\alpha)$, the particle density decays with system size. **(b)** The hole density in the system, given by $1 - \gamma$ is plotted as function of chemical potential at zero temperature. The vertical line corresponds to $\mu = 2\eta(\alpha)$. For $\mu > 2\eta(\alpha)$, the particle density decays with system size. For the plots, the bath spectral functions are chosen to be $\mathfrak{J}_1(\omega) = \mathfrak{J}_N(\omega) = \Gamma \sqrt{1 - (\frac{\omega}{\Lambda})^2}$, with $\Lambda = 8$, $\Gamma = 10$.

of both particles and holes. Here we explicitly check this. The particle density in the system is defined as

$$\gamma = \frac{1}{N} \sum_{\ell=1}^N \langle \hat{c}_{\ell}^{\dagger} \hat{c}_{\ell} \rangle. \quad (\text{S28})$$

The occupation at ℓ th site in NESS is given in terms of the NEGF as

$$\langle \hat{c}_{\ell}^{\dagger} \hat{c}_{\ell} \rangle = \int_{-\Lambda}^{\mu} \frac{d\omega}{2\pi} \left[|\mathbf{G}_{1\ell}(\omega)|^2 \mathfrak{J}_1(\omega) + |\mathbf{G}_{N\ell}(\omega)|^2 \mathfrak{J}_N(\omega) \right], \quad (\text{S29})$$

where $-\Lambda$ is the minimum energy of the band of the bath. We numerically calculate γ and check its behavior with μ and N . When there is a sub-extensive number of particles in the system, γ decays with N , which happens for $\mu < -2\zeta(\alpha)$. When there is an extensive number of particles in the system, γ is independent of N , which happens for $\mu > -2\zeta(\alpha)$. When there is a sub-extensive number of holes in the system, $1 - \gamma$ decays with N , which happens for $\mu > 2\eta(\alpha)$, while if there is an extensive number of holes in the system, $1 - \gamma$ is independent of system-size, which happens for $\mu < 2\eta(\alpha)$.